新能源动力技术

文章编号: 1001－2060(2010)02－0226－04

依托高楼的太阳能热气流电站系统的 CFD模拟

周　艳, 李洁浩, 李庆领
(青岛科技大学 机电工程学院, 山东 青岛 266042)

摘　要: 设计了一种依托高楼的太阳能热气流电站, 建立了相应的数学模型。利用 Fluent软件对该系统的流场及温度场进行了数值模拟, 并对电站结构进行了优化设计。模拟结果表明: 随着烟囱高度的增加, 烟囱内气流的温度不断上升, 在出口处由于回流的影响温度稍有下降, 气流速度不断增大, 气流的压力分布先减小后增加。由于平板集热器的加热作用使烟囱内气流的温度分布不均匀, 设计中可将平板型储热器换为带有肋片扩展表面的储热器, 并对烟囱与扩压管联接处采用流线形联接进行过渡, 以减少此处的流动阻力。同时, 设计一个收缩型的烟囱出口, 以保证电站系统产生较大的抽力, 从而提高电站系统的能量转换率。

关　键　词: 太阳能热气流电站; 流场; CFD; 烟囱高度; 优化设计

中图分类号: TM615; O354　　文献标识码: A

引　言

能源是国民经济发展的重要基础, 也是人们生产和生活的重要物质基础保障, 但随着我国经济的持续快速发展, 能源问题已经成为制约经济与社会发展的“瓶颈”之一。由德国施莱德教授在 1978年提出的太阳能热气流发电技术其发电成本低、不需冷却水、设计简单, 施工方法和建筑材料均可在当地获得、电站系统仅涡轮机、传动装置和发电机是电站的运动部分, 运行非常可靠, 不需燃料等优点, 被许多能源专家看好[1~3]。

但原始结构的太阳能热气流发电技术至今仍没有被广泛应用, 主要因为该技术存在以下缺点: 集热棚很容易被尘土盖上, 不易清洗, 易被破坏; 超高烟囱存在防风防震安全问题; 大结构涡轮发电机组在经济上不合算[4~5]; 另外, 原始结构的太阳能热气流电站集热棚的占地面积较大, 只能建于沙漠及荒漠化等人稀地广的地区, 对于太阳能资源同样丰富的城市地区不适用, 这就大大限制了太阳能热气流发电技术的应用范围。为了扩大太阳能热气流发电技术的应用领域, 研究设计了一种依托高楼而建的新型太阳能热气流电站。

1　依托高楼的太阳能热气流电站装置

图 1为依托高楼而建的新型太阳能热气流电站结构。

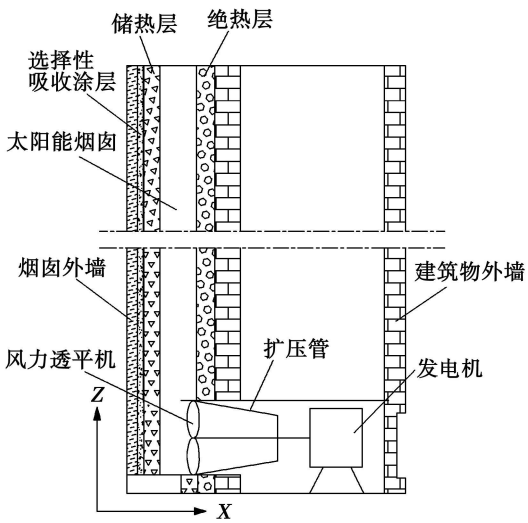

图 1　依托高楼的太阳能热气流电站结构示意图

在图 1所示的模型中, 各部件的材料选择如表 1所示。

这种新型太阳能热气流电站主要由内涂选择性吸收涂层的透明材料 (图 1中的烟囱外墙与选择性吸收涂层与储热层合称为集热器)依托高楼向阳墙面搭建而成, 在集热器与高楼墙面之间形成的空气向上流动的通道称为太阳能烟囱。空气在烟囱中至

收稿日期: 2009－03－12　修订日期: 2009－06－01
基金项目: 山东省自然基金资助项目(Z2008F05); 山东省教育厅基金资助项目(J08LA13)
作者简介: 周　艳(1973－), 女, 贵州贵阳人, 青岛科技大学讲师.

下而上的吸收太阳热能,温度不断上升,密度不断减小,这就加强了空气向上浮起的拽升引射流动,并将太阳热能转换成空气流动的动能,而从建筑物底部源源不断补充的冷空气经过扩压管的扩压后推动风力透平机组旋转做功[6]。

表 1　材料特性

	密度 ρ/kg·m^{-3}	定压比热 c_p/J·(kg·K)$^{-1}$	导热系数 λ/W·(m·K)$^{-1}$	粘性系数 μ/kg·(m·s)$^{-1}$	热膨胀系数 β/K^{-1}
玻璃	2 500	837.4	0.75	—	—
空气	1.205	1 005.43	0.025 9	1.81e−05	0.003 4
绝热材料(聚乙烯泡沫)	100	1 380	0.047	—	—

太阳能为一种间歇式能源,其辐射受到昼夜、季节以及雨雪天气等因素的影响,表现为间断性和不稳定性,解决这一问题的关键是采用可靠的、性能优良的储热装置,它可以在获得太阳能期间进行储热,在太阳能间断期,将所储热量释放供人们使用。因此,为保证电站系统的连续运转,系统设有储热装置,在储热装置与高楼墙体之间设置了绝热层,以防止储热层与高楼室内空气的热量传递。这种设计将原始设计中占地面积较大的集热棚与烟囱集成为一体,形成一种依托高楼的新型太阳能热气流电站。与传统的太阳能热气流电站相比,这种新型的太阳能热气流发电系统具有以下特点:

(1)将原来只适用于荒漠及沙化地区的太阳能热气流技术用于城市地区,扩大了太阳能热气流发电技术的应用范围。

(2)烟囱结构简单,用材单一,同时依托建筑物墙体搭建,受力情况较好,易于搭建。

(3)太阳能烟囱内的空气流动可同时改善建筑物内的通风情况,提高室内的空气质量。

(4)绝热层的设置可防止建筑物与储热设备之间的热量交换,达到夏天阻热、冬天保暖的作用。

2　数学模型

为了简化计算,同时又能得到较为合理的结果,采用基本假设来简化模型:(1)过程是稳定的,太阳辐射强度和环境气温等条件不随时间变化,体系内空气的运动参数和状态参数也不随时间发生改变;(2)忽略烟囱的散热损失;(3)忽略空气渗透;(4)各部件的材料特性与温度无关;(5)烟囱内空气变化采用 Boussinesq假定。控制微分方程包括连续性方程、动量方程和能量守恒方程[7~11]。

对于稳态可压缩流体,连续性方程为:

$$\frac{\partial(\rho u)}{\partial x}+\frac{\partial(\rho v)}{\partial y}+\frac{\partial(\rho w)}{\partial z}=0 \qquad (1)$$

通用控制微分方程为:

$$\frac{\partial(\rho u\phi)}{\partial x}+\frac{\partial(\rho v\phi)}{\partial y}+\frac{\partial(\rho w\phi)}{\partial z}+=\frac{\partial}{\partial x}\left(\Gamma_\phi\frac{\partial\phi}{\partial x}\right)+\frac{\partial}{\partial y}\left(\Gamma_\phi\frac{\partial\phi}{\partial y}\right)+\frac{\partial}{\partial z}\left(\Gamma_\phi\frac{\partial\phi}{\partial z}\right)+S_\phi \qquad (2)$$

式中:ϕ—通用变量,分别代表 u、v、w、k、ε和 T;Γ_ϕ—扩散项系数;S_ϕ—源项。当 ϕ赋予特定含义时,Γ和 S有相应的特定值或代表式。

对于 u、v、w、T、K、ε和 T的广义扩散系数 Γ_ϕ分别为:

u、v、w: $\Gamma_\phi=\mu+\mu_t$,　　T: $\Gamma_\phi=\frac{\mu}{p_r}+\frac{\mu_t}{\sigma_T}$

k: $\Gamma_\phi=\mu+\frac{\mu_t}{\sigma_k}$,　　ε: $\Gamma_\phi=\mu+\frac{\mu_t}{\sigma_\varepsilon}$

对于 u、v、w、T及 k、ε的源项分别为:

u: $S_\phi=-\frac{\partial p}{\partial x}+\frac{\partial}{\partial x}\left(\mu_{eff}\frac{\partial u}{\partial x}\right)+\frac{\partial}{\partial y}\left(\mu_{eff}\frac{\partial v}{\partial x}\right)+\frac{\partial}{\partial z}\left(\mu_{eff}\frac{\partial w}{\partial x}\right)$

v: $S_\phi=-\frac{\partial p}{\partial y}+\frac{\partial}{\partial x}\left(\mu_{eff}\frac{\partial u}{\partial y}\right)+\frac{\partial}{\partial y}\left(\mu_{eff}\frac{\partial v}{\partial y}\right)+\frac{\partial}{\partial z}\left(\mu_{eff}\frac{\partial w}{\partial y}\right)$

w: $S_\phi=-\frac{\partial p}{\partial z}+\frac{\partial}{\partial x}\left(\mu_{eff}\frac{\partial u}{\partial z}\right)+\frac{\partial}{\partial y}\left(\mu_{eff}\frac{\partial v}{\partial z}\right)+\frac{\partial}{\partial z}\left(\mu_{eff}\frac{\partial w}{\partial z}\right)+\rho g\beta(T-T_\alpha)$

k: $S_\phi=G_K+G_b-\rho\varepsilon$

ε: $S_\phi=\frac{\varepsilon}{k}[C_1(G_K+G_B)-C_2\rho\varepsilon]$

T: $S_\phi=0$

$k-\varepsilon$方程中的湍流动能产生项 G_k为:

$$G_k=\mu_t\left\{2\left[\left(\frac{\partial u}{\partial x}\right)^2+\left(\frac{\partial v}{\partial y}\right)^2+\left(\frac{\partial w}{\partial z}\right)^2\right]+\left(\frac{\partial u}{\partial y}+\frac{\partial v}{\partial x}\right)^2+\left(\frac{\partial u}{\partial z}+\frac{\partial w}{\partial x}\right)^2+\left(\frac{\partial v}{\partial z}+\frac{\partial w}{\partial y}\right)^2\right\}$$

浮升力产生项 G_b为:

$$G_b=\beta g\frac{\mu_t}{Pr_t}\cdot\frac{\partial T}{\partial z}$$

湍流粘性系数为：$\mu_t=\rho\cdot C_\mu\cdot\frac{k^2}{\varepsilon}$，$\mu_{eff}=\mu+\mu_t$

其中，$\mu=10^{-6}$ kg/(m·s)；k—ε方程中其它系数取值为：

$C_\mu=0.09$，$C_1=1.44$，$C_2=1.92$，$\sigma_k=1.0$，$\sigma_\varepsilon=1.3$，$Pr=0.7$，$\beta=3.33\times10^{-3}$/K。

以上各式中符号分别表示：u—水平方向速度；v—纵向方向速度；w—垂直方向速度，m/s；k—湍流动能；ε—湍流动能耗散率；T_a—环境温度，K。

3 数值计算及结果分析

采用 GAMBIT软件按照图 1建模，采用分块网格技术对研究对象进行网格划分，采用 Fluent6软件对依托高楼的太阳能热气流电站的数学模型进行三维稳态数值求解，对于气流的湍流计算采用标准 k—ε模型。在对守恒方程选用离散格式时，对于动量方程采用一阶迎风格式，用 Simple方法来处理压力—速度的耦合。为便于求解离散方程，在不影响数值精度的前提下，对能量方程、湍动能方程和湍动能耗散方程也都采用了一阶迎风格式。计算时边界条件为：环境压力0.1MPa，环境温度 300 K，同时集热板表面采用第二类边界条件，即 $q=C$，而储热层与流体之间采用第三类边界条件，即 $q=h\cdot(t-t_w)$，其余墙体表面均为绝热边界条件以及固体壁面无滑移条件。

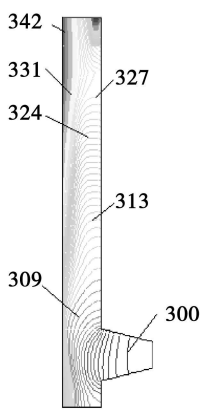

图 2 电站系统温度分布(K)

图 2、图 4及图 5为太阳辐射强度为 800 W/m²时，烟囱厚度 X=2 m，宽度 Y=6 m，高度 Z=30 m时，电站系统空载运行时的温度场分布和流场分布的模拟结果。

图 2是烟囱内气流的温度分布图。由图可知：当 27 ℃的空气进入系统时，其温度升高值在 40 ℃以上，这样的温升可使空气的密度有较大的改变，从而达到使气流引射向上流动的效果。另外，从图 2中还可以看出，气流温度随着烟囱高度的增加而逐渐升高，在同一水平面中，靠近集热器处气流有较大的温度梯度。这是因为：(1)由于本结构中烟囱是由平板式集热板搭建而成，集热板吸收太阳热能后，通过对流换热的方式加热烟囱内的空气，随着烟囱高度不断增加，空气在烟囱内不断吸收热量，温度也不断上升。(2)由于集热板吸收热量通过对流换热的方式加热靠近集热板的空气，而后被加热的空气通过导热的方式将热量进一步传递给远离集热板的空气，由于空气导热能力较差，因此在靠近集热板处空气会出现较大的温度梯度。(3)由于烟囱出口存在回流现象，使烟囱出口靠近内壁处气流温度有一定的下降。

为使烟囱气流温度分布均匀，设计了一种新型的集热板与储热装置，该结构中储热器具有肋片型式的扩展表面，其结构如图 3所示。

采用此结构可使气流在烟囱通道内有多个表面与热流体进行对流换热，因此气流温度分布均匀，可较大程度地改善了远离集热板壁面处气流的滞流情况。

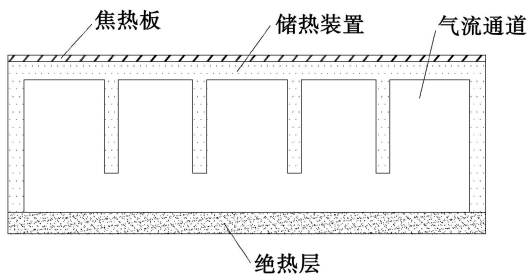

图 3 改进的储热装置横截面结构示意图

电站系统内部气流的速度分布如图 4所示。从图 4中可以看到，烟囱内气流速度变化不太显著，且分布较为均匀。从 X—Z截面速度分布图看出，在流道中心且靠近烟囱出口处气流出现最大流速，说明由于气体粘性的存在而使气流在贴近烟囱壁面处存在较大的速度梯度；另外，烟囱与扩压管连接处速度梯度较大，将会产生较大的能量损失。对于该部位，在设计时采用流线形联接进行过渡，以减少此处的流动阻力。在 Y—Z截面上气流速度总体变化不大，在同一水平面上的流速较均匀，这是因为：由于

Y— Z截面上在同一高度的水平面上烟囱内气流吸热量是相等的。

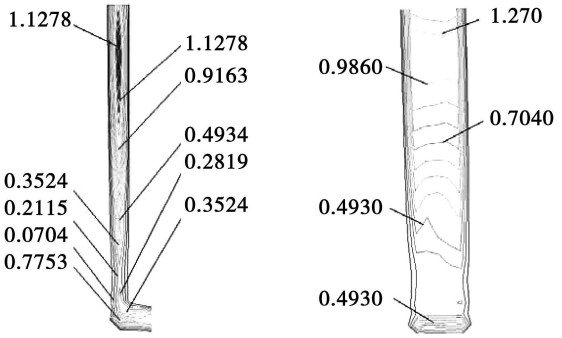

图 4　烟囱内气流的速度分布图 (m/s)

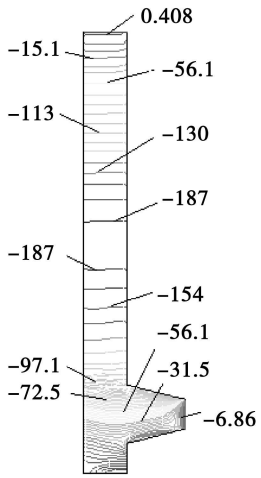

图 5　烟囱内气流压力场 (Pa)

由于烟囱抽力及热压作用,气流在烟囱内的压力分布理论上应该是逐渐减小。而由图 5可见 (图中压力为表压),系统内部随着烟囱高度的增加,气体压力先减小后增加,分析原因如下:由于在建模时没有考虑烟囱出口处的设计,气流直接从面积为 12 m²的烟囱出口排入大气环境,为保证烟囱内气流顺利从烟囱出口排向大气环境,烟囱内气流的压力在出口处必须高于大气环境压力,因此烟囱内气流的压力在烟囱中部后逐渐上升。为了使烟囱内气流的压力分布更合理,电站系统能产生较大的抽力,在设计烟囱出口时,应考虑将出口面积尽可能减小,设计一个收缩型的烟囱出口。另外,从图 5中还可看出,在扩压管与烟囱联接区域,压降比较明显,显然该区域的压降越大,能量利用率越高。

4　结　论

(1)利用 Fluent软件对依托高楼的太阳能热气流电站系统中气流的温度分布、流动状况及压力场进行了数值模拟,并依据数值模拟结果对原始设计的依托高楼的太阳能热气流电站的结构进行了优化设计,为电站系统实验平台的建设提供理论依据。

(2)随着烟囱高度的增加,烟囱内气流的温度不断上升,在出口处由于回流的影响温度稍有下降,气流速度不断增大,气流的压力分布先减小后增加。

(3)由于平板集热器的作用使烟囱内气流的温度分布不均匀,因此在设计中可将平板型储热器设计为带有肋片扩展表面的储热器,以此增大集热板的加热空气的面积,使空气吸收更多的太阳辐射能;

(4)对烟囱与扩压管联接处采用流线形联接进行过渡,以减少此处的流动阻力;并设计一个收缩型的烟囱出口,以保证电站系统产生较大的抽力,从而使电站系统的能量转换率提高。

参考文献:

[1] SCHLAICH J. The solar chimney: Electricity from the sun[M]. Germany: Maurer C, editor. Geislingen, 1995.

[2] ROBERT R. Spanish solar chimney nears completion[J]. MPS Review, 1981(6): 21—23.

[3] HAAF H, FRIEDRICH K, MAYER G, et al. Solar chimney: Part a: Principle and construction of the pilot plant in Manzanares[J]. Int J of Solar Energy, 1983(2): 3—20.

[4] 黄素逸. 太阳能热气流电站系统的研究进展[J]. 东莞理工学院学报, 2006, 13(4): 10—14.

[5] 杨家宽,李　劲,肖　波,等. 太阳能烟囱发电新技术[J]. 太阳能学报, 2003(4): 565—569.

[6] 王宝瑞. 太阳能引射流空气流体发电原理[EB/OL]. 中国科技论文在线. http://www.paper.edu.cn.

[7] BERNARDES M A, DOS S. Thermal analyses of a solar chimneys[M]. Dissertation, Universidade Federal de Minas Gerais, Belo Horizonte, 1997.

[8] CLETO AFHMSP, ARMANDO OLIVEIRA. A solar chimney: simulation and experiment[J]. Energy Dings, 2000, 32: 71—79.

[9] 周新平,杨家宽,肖　波,等. 太阳能烟囱发电装置的 CFD模拟[J]. 可再生能源, 2005(4): 8—11.

[10] 刘　伟,明廷臻,杨　昆,等. MW级太阳能热气流电站传热和流动特性研究[J]. 华中科技大学学报(自然科学版), 2005, 33(8): 5—7.

[11] BERNARDES MAS, VOB A, WEINREBE G. Thermal and technical analyzes of solar chimneys[J]. Solar Energy, 2003, 75: 11—524.

content of the flying ash will be the highest when the initial oxygen concentration is 21%. It will drop by a great margin when the initial oxygen concentration increases to 30% ~40%. Thus, 30% initial oxygen concentration is considered as a comparatively rational choice for the oxygen-enriched combustion. Key words: utility boiler; flame temperature; oxygen concentration; O_2/CO_2 atmosphere; NOx; numerical simulation

1 000 MW机组锅炉氮氧化物排放影响的试验研究 = Experimental Study of the Influence of NO_x Emissions from the Boiler of a 1000 MW Power Plant[刊, 汉] / GAO Xiao-tao(Jiangsu Electric Power Test and Research Co., Ltd., Nanjing, China, Post Code: 211102), HUANG Lei, ZHANG En-xian(Jiangsu Frontier Electric Power Technology Co. Ltd., Nanjing, China, Post Code: 211102), ZHANG Ming-yao(College of Energy Source and Environment, Southeast University, Nanjing, China, Post Code: 210096) // Journal of Engineering for Thermal Energy & Power. — 2010, 25(2). — 221 ~225

On the basis of the on-site test methods for combustion adjustment, a systematic study and analysis was performed of the NOx emissions characteristics of a 1 000 MW ultra-supercritical tangentially-fired boiler in a power plant along with its influencing factors. In the light of the operation characteristics of the boiler combustion system, mainly studied were such influencing factors as the oxygen quantity, load, burn-out air quantity (including additional air and over-fired air), air quantity and air distribution mode for burners in the main combustion zone, ball mill operation combination mode, swaying angle of burners and coal ranks etc. The test and research results show that as an air staged combustion in the furnace is adopted, it is decisive that the change of coal quality will remarkably affect the concentration of NOx emissions. The change of the oxygen quantity during the operation is an important factor influencing the concentration of NOx emissions. With an increase of the oxygen quantity, the concentration of NOx emissions from the boiler will increase linearly. The boiler load is also a major factor influencing the concentration of NOx emissions. The extent of such an influence depends on the boiler load and the operating oxygen quantity during the corresponding load. The swaying of the burner spout and the change of the ball mill operation mode will exercise a significant influence on the concentration of NOx emissions from the boiler. Relative to the influence exerted by the above-mentioned factors, under the condition that a large amount of burn-out air is maintained to realize an air staged and fractional combustion, the change of the primary and secondary air distribution in the main combustion zone has a weak influence on the concentration of NOx emissions. Key words: ultra-supercritical boiler; low NOx combustion; NOx emissions; burner air feed; air distribution mode; operating factors

依托高楼的太阳能热气流电站系统的 CFD模拟 = CFD (Computational Fluid Dynamics) Simulation of a Solar Energy Hot Airstream Power Plant System Installed in a High Building[刊, 汉] / ZHOU Yan, LI Jie-hao, LI Qing-ling (College of Electromechanical Engineering, Qingdao University of Science and Technology, Qingdao, China, Post Code: 266042) // Journal of Engineering for Thermal Energy & Power. — 2010, 25(2). — 226 ~229

Designed was a solar energy hot airstream power plant installed in a high-rise with a corresponding mathematical model being established. By using software Fluent, a numerical simulation was performed of the flow and temperature fields in the power plant system under discussion. Moreover, the power plant configuration also underwent an optimized design. The simulation results indicate that with an increase of the smoke stack height, the airstream temperature in the smoke stack will ceaselessly rise and drop slightly at the outlet as influenced by the return flow. With the airstream velocity ever increasing, the airstream pressure distribution will first decrease and then increase. In the meantime, as the airstream is being heated by a plate-type heat collector, the airstream temperature distribution in the smoke stack is not homogeneous. The plate type heat accumulator can be designed as one with finned ex-

tended surface to form a heat storage unit. The connection between the smoke stack and the pressure diffusion tube can be streamlined to form a transition, thus reducing the drag force at the above location. At the same time, a convergent smoke stack outlet can be designed to secure a relatively big suction head for the power plant system, thereby enhancing the energy conversion rate of the system in question. Key words: solar energy, hot airstream power plant, flow field, CFD (computational fluid dynamics), smoke stake height, optimized design

直接碳燃料电池活性炭制备的实验研究 = Experimental Study of Active Carbon Preparation for Direct Carbon Fuel Cells[刊, 汉] / ZHANG Ju-bing, ZHONG Zhao-ping, GUO Hou-kun, JIN Bao-sheng (Thermal Energy Engineering Research Institute, Southeast University, Nanjing, China, Post Code: 210096) // Journal of Engineering for Thermal Energy & Power. — 2010, 25(2). — 230 ~ 233

With KOH serving as an activation agent, experimentally studied was the active carbon prepared from oak wood sawdust by adopting a chemical activation method. The influence of the activation temperature, alkali/carbon ratio and activation time on the specific surface area of the active carbon was investigated. On this basis, the optimum operating condition for active carbon preparation was obtained. Subsequently, HNO_3 soaking and nickel acetate loading were used successively to the active carbon under the above-mentioned conditions. It has been found that the specific surface area of the active carbon prepared under the optimum operating condition is 1 967 m^2/g. HNO_3 soaking can increase the variety and content of oxygen-containing functional groups on the surface of the active carbon and decrease the ash content of the active carbon to a relatively big extent. After a pad has been added to the active carbon by using nickel acetate, the volumetric resistivity of the active carbon will drop greatly. Key words: active carbon, specific surface area, volumetric resistance rate, oxygen-containing functional group, direct carbon fuel cell

混燃的稻壳飞灰特性的试验研究 = Experimental Study of the Flying Ash Characteristics of Mixed Burned Rice Husks[刊, 汉] / YAN Wei-ping, LIU Xu-ao (Education Ministry Key Laboratory on Power Plant Equipment Condition Monitoring and Control, College of Power and Mechanical Engineering, North China University of Electric Power, Baoding, China, Post Code: 071003), SHEN Ye, YUAN Guang-fu (Guodian Changyuan Electric Power Shareholding Co. Ltd., Wuhan, China, Post Code: 430000) // Journal of Engineering for Thermal Energy & Power. — 2008, 25(2). — 234 ~ 237

On a 300 MW pulverized coal-fired boiler in a power plant, a mixed burning test was conducted of rice husks. The microscopic-morphopgical appearance, chemical properties and pore structure etc. of the ash produced by the rice husks in the mixed burning were tested and analyzed. The authors have mainly concluded that quartz, scale quartz and cristobalite in the crystal form predominate in the rice husk-produced ash physical phase and there exists a small amount of mullite crystal. The rice husk-formed ash appears in the form of irregular slice-shaped ash particles with large diameters. The convex surface of the husk-formed ash is of a wave shape in a melt state accompanied by a small number of bubble pores. The concave surface of the husk ash is abundant in pore structures. In the analytic results of constant elements, the content of SiO_2 in the husk-formed ash can be as high as 97.42%. However, the content of Al_2O_3, K_2O and CaO in the ash is low. The average diameter of the pores in the husk-formed ash is 9.704 nm, mercury filled volume amounts to 0.181 1 cm^3/g and the specific surface area of the sample totals 74.633 2 m^2/g. The husk-formed ash segregated from the fly ash after a co-firing can be used as porous materials. Key words: pulverized coal-fired boiler, rice husk burning, physical phase, co-firing, flying ash characteristics